



1 Tectonostratigraphy of the Mérida Massif reveals a new
2 suture zone exposure in SW Iberia

3

4 **Rubén Díez Fernández^{1*}, Ricardo Arenas², Esther Rojo-Pérez², Sonia Sánchez**
5 **Martínez², José Manuel Fuenlabrada³**

6

7 *¹Departamento de Geodinámica, Estratigrafía y Paleontología, Universidad*
8 *Complutense de Madrid, 28040 Madrid, Spain*

9 *²Departamento de Mineralogía y Petrología, Universidad Complutense de Madrid,*
10 *28040 Madrid, Spain*

11 *³Unidad de Geocronología (CAI de Ciencias de la Tierra y Arqueometría), Universidad*
12 *Complutense de Madrid, 28040 Madrid, Spain*

13

14 *Corresponding author: rudiez@ucm.es

15

16 **ABSTRACT**

17 Dividing a crystalline basement into tectonostratigraphic units, along with the recognition
18 of the nature of their boundaries (primary vs. tectonic), are essential steps to identify
19 major tectonic slices involved in orogeny. The Neoproterozoic and Paleozoic rocks of the
20 Mérida Massif (SW Iberia) have been grouped into five tectonostratigraphic units
21 according to their structural position, continental or oceanic crust affinity, and equivalent
22 tectonometamorphic evolution. Each unit is separated from the rest ones by either crustal-
23 scale thrusts and/or extensional detachments. The lowermost unit (Magdalena Gneisses;
24 lower plate) has continental crust affinity, and rest below a variably strained and



25 metamorphosed mafic-ultramafic ensemble, referred to as the Mérida Ophiolite (suture
26 zone). The Neoproterozoic Montemolín Formation of the Serie Negra Group constitutes
27 a unit with continental crust affinity (Upper Schist-Metagranitoid Unit; upper plate)
28 located on top of the Mérida Ophiolite. A carbonate-rich succession (Carija Unit)
29 occupies the uppermost structural position. Structural and isotopic data suggest that the
30 suture zone depicted by the Mérida Ophiolite and the tectonic piling and main foliation
31 of the Neoproterozoic and Cambrian units were formed during the Cadomian Orogeny.
32 Superimposed shortening during the late Paleozoic formed a train of upright to NE-
33 verging folds and thrusts that affected the Cadomian suture zone and juxtaposed it onto
34 Ordovician strata (fifth tectonostratigraphic unit) during the Variscan Orogeny. Cenozoic
35 contraction during the Alpine Orogeny formed SW-directed thrusts in an intraplate
36 setting. The Mérida Ophiolite represents a new Cadomian suture zone exposure of the
37 Iberian Massif, but its root zone is yet to be identified. This suture zone exposure seems
38 to share a far-travelled nature with other Cadomian and Variscan suture zone exposures
39 in Iberia, making the latter a piece of continental lithosphere built at the expense of
40 allochthonous terranes transferred inland from peri-Gondwana onto mainland Gondwana,
41 both during the Neoproterozoic-Cambrian and the Devonian-Carboniferous.

42

43 **Keywords:** Cadomian tectonics; Cadomian allochthons; Cadomian suture; Ophiolite;
44 Variscan tectonics; SW Iberian Massif

45

46 1. INTRODUCTION

47 Bedrock mapping of regions featured by a rich variety of rocks may result in
48 contrasting outcomes depending on lithological grouping criteria. Establishing coherent
49 lithological groups to be mapped is essential. Classical criteria to divide crystalline



50 basement bedrock include: (i) structural position at regional scale, (ii) continental,
51 oceanic or transitional crust affinity, and (iii) equivalent tectonometamorphic evolution.
52 Such approach leads to the establishment of what is usually referred to as the
53 tectonostratigraphy of a region, a practical concept that gathers compositionally complex
54 rock sequences layered after penetrative deformation affecting one or more sections of
55 the lithosphere, each of which would represent an independent tectonostratigraphic unit.
56 This workflow has advantages and drawbacks of its own, but allows identifying major
57 geological features and helps set the base for future, more oriented, research. Grouping
58 of contrasting lithologies makes detailed time-resolved geodynamic reconstructions
59 based on petrological aspects more difficult, but on the other hand it favors recognition
60 of terranes (e.g., major tectonic blocks) by acknowledging their internal complexity. This
61 purpose-oriented method is particularly useful to identify continental blocks intervening
62 in a suture zone, and is actually the basis for widely accepted ideas in tectonic
63 reconstructions, such as the ophiolite concept.

64 Here we present a new simplified geological map and cross-section of the Mérida
65 Massif aimed to distinguish its main tectonostratigraphic units and their relationships.
66 Lithological ensembles for each unit have been grouped according to criteria cited above.
67 The resulting tectonostratigraphy provides light into a nappe structure that had remained
68 unnoticed for the region, despite large scale thrusting events in SW Iberia have been
69 claimed for Variscan models (Azor et al., 1994; Díez Fernández and Arenas, 2015;
70 Ribeiro et al., 2010) and Cadomian tectonics (Díez Fernández et al., 2019; Abalos et al.,
71 1991). It also adds another ophiolite and suture zone exposure to the set that features the
72 Iberian Massif, thus strengthening the notion of the Iberian domain as a region built after
73 numerous suturing processes throughout geological history.

74



75 2. GEOLOGICAL SETTING

76 The Iberian Massif constitutes the southernmost exposure of the Variscan Orogen
77 in Europe (Fig. 1), which resulted from the progressive collision of Gondwana, Laurussia
78 and their respective pericontinental terranes during the Devonian and Carboniferous
79 (Simancas et al., 2013; Martínez Catalán et al., 2009; Ribeiro et al., 2007; Díez Fernández
80 et al., 2016). Yet, the current structure of the Iberian Massif is the result of three orogenic
81 cycles. Gondwana was affected by long-lived subduction under its periphery during the
82 Neoproterozoic and Lower Paleozoic (Linnemann et al., 2007; Quesada, 1990; Pereira et
83 al., 2007; Eguíluz et al., 2000; D’Lemos et al., 1990; Nance et al., 1991; Chantraine et al.,
84 2001), its northern paleomargin bearing abundant evidence of arc-related magmatism
85 (Bandrés et al., 2004; Henriques et al., 2015; Dorr et al., 2002; Drost et al., 2004; Rubio-
86 Ordóñez et al., 2015), basin development in active settings (Rojo-Pérez et al., 2019;
87 Fuenlabrada et al., 2012; Fuenlabrada et al., 2016; Linnemann et al., 2000; Linnemann et
88 al., 2007; Fernández-Suárez et al., 2013; Pereira, 2015), and contractional and extensional
89 deformation (Díez Fernández et al., 2019; Expósito et al., 2003; Simancas et al., 2004;
90 Eguíluz et al., 2000; Bandres et al., 2002; Kröner et al., 2000; Strachan and Taylor, 1990;
91 Díaz García, 2006; Balé and Brun, 1989), all of which are collectively referred to as
92 Cadomian Orogeny (cycle). It is well-established that the external section of Gondwana
93 facing such subduction was involved in the Variscan cycle, whose onset and culmination
94 may correspond to an extensional event that led to the opening of oceanic basins (e.g.,
95 Rheic Ocean; Nance et al., 2010; Linnemann et al., 2007), and the raise of the Variscan
96 Orogen after their suturing (Matte, 1991; Martínez Catalán et al., 2009; Ballèvre et al.,
97 2009; Franke, 2000), respectively. The Iberian Massif contains Cenozoic mountain
98 ranges formed during the Alpine cycle (e.g., de Vicente and Vegas, 2009). Some of them
99 occur at the boundaries of the Iberian micro-plate (e.g., Pyrenees, Betics), while others



100 occupy intra-plate positions. Both are the result of plate tectonics in the Mediterranean
101 domain as well as of distributed strain upon Africa-Europe convergence (Dewey et al.,
102 1989; Jolivet et al., 2008; de Vicente et al., 2018).

103 The Mérida Massif is located in the SW part of the Iberian Massif (Fig. 2).
104 Previous studies have suggested that its composition and current structure is the result of
105 Cadomian, Variscan, and Alpine tectonics (Bandrés, 2001; Gonzalo, 1987, 1989; Insúa
106 Márquez et al., 2003). This massif includes an extensive exposure of Neoproterozoic and
107 Lower Paleozoic rocks (Fig. 3), and represents a good opportunity to study Cadomian
108 tectonics and the interference of subsequent orogenic cycles over Cadomian imprint.
109 Mapping of its bedrock geology has provided rather different outcomes over the years
110 (Insúa Márquez et al., 2003; Bandrés, 2001; Gonzalo, 1987; Roso de Luna and Hernández
111 Pacheco, 1950). Although poorness of exposure may explain some variation, most of it
112 seems to derive from contrasting criteria followed during mapping. The Mérida Massif,
113 although relatively small in size, is characterized by a significantly rich variety of rocks,
114 making it difficult to establish coherent lithological groups to be mapped if not oriented
115 to a purpose. Deformation in this area includes the development of foliations, folds, faults,
116 and shear zones, some of which are coeval to pervasive metamorphism (Gonzalo, 1987,
117 1989; Bandrés, 2001; Bandrés et al., 2000).

118

119 **3. TECTONOSTRATIGRAPHY**

120 In this section, we will provide a brief description of the main lithological
121 associations we have established in the Mérida Massif. Grouping is aimed to the
122 recognition of major tectonic blocks intervening in Cadomian and Variscan tectonics.
123 Rocks included into each tectonostratigraphic unit meet the following grouping criteria,
124 and they are different from those gathered into other units for the same reasons: (i) similar



125 structural position at regional scale, (ii) the ensemble shows either continental or oceanic
126 crust affinity, (iii) equivalent tectonometamorphic evolution, and (iv) they are separated
127 from other units by either a major mechanical boundary (i.e., fault or ductile shear zone)
128 or a major stratigraphic discontinuity (e.g., discordance). Age of protoliths alone was not
129 taken as a grouping criteria, because the amalgamation of two tectonic blocks may
130 juxtapose rocks of similar age located at each block. Descriptions are given following
131 reverse chronological order according to their (meta-) sedimentary strata. In case bedding
132 and age constrains are lacking, overlying units (as indicated by their main foliation) will
133 be described first.

134

135 **3.1. Cenozoic cover**

136 The crystalline basement of the Mérida Massif is discordantly covered by a wide
137 variety of Cenozoic sedimentary rocks. Since Cenozoic processes are not the focus of this
138 contribution, no distinction has been made in the geological map between sequences of
139 different age and composition. Previous works have divided this Cenozoic cover into
140 informal units according to their age (Miocene through to Holocene), location, and
141 sedimentary environment (Insúa Márquez et al., 2003).

142 The oldest Cenozoic deposit is represented by Miocene conglomerates and arkosic
143 sandstones, followed by sandstones and conglomerates, and then red silt and clay and
144 minor sandstones. This continental series is succeeded by Miocene arkosic sandstones,
145 which are then covered by a Pliocene-Pleistocene succession of conglomerates,
146 sandstones and silt. Other Pleistocene and Holocene deposits include carbonated deposits
147 (caliche), carbonated crusts, glacia deposits (irregular pebbles, gravel, and minor silt),
148 fluvial terraces (rounded conglomerates, sandstones, and silt), alluvial fans, and aeolian
149 sands.



150

151 **3.2. Ordovician strata**

152 The youngest sedimentary series that is now exposed as metamorphic rocks in the
153 study area corresponds to a succession of meta-sandstones, meta-conglomerates,
154 quartzites, and slates that occurs to the north of the Mérida Massif (Fig. 3). The series is
155 cut by a major fault, so its basal section is not exposed in the study area. The lower part
156 exposed consists of coarse-grained meta-sandstones (quartz-rich micro-conglomerates),
157 which are covered by quartzites and orthoquartzites that alternate with slates. Quartzite
158 beds are thinner upwards while slates become more abundant. This part of the series has
159 been ascribed to the Early Ordovician (Tremadocian-Floian), and is considered a SW
160 Iberian correlative to the (Arenig) Armorican quartzite (Insúa Márquez et al., 2003;
161 Gutiérrez-Marco et al., 2002). The series culminates with black slates and minor layers
162 of black quartzites exposed within, whose age has been considered to be Middle
163 Ordovician (Llanvirn-Llandeil) (Insúa Márquez et al., 2003).

164

165 **3.3. Cambrian carbonate-rich series: Carija Unit**

166 This unit gathers a carbonate-rich, meta-sedimentary succession of variably
167 strained rocks that is exposed northwest of Merida town (Fig. 3), around the Carija hill.
168 Strain is particularly concentrated along its basal boundary and decreases progressively
169 upwards. The lower part consists of black calc-schists that rest below a series in which
170 fine-grained, banded grey-white marbles alternate with fine-grained dark grey-light grey
171 dolomitic marbles and yellow-brown marbles. This series has been ascribed to the Early
172 Cambrian (Insúa Márquez et al., 2003), and considered correlative to other carbonate-rich
173 Early Cambrian successions of SW Iberia (e.g., Sánchez-García et al., 2010).

174



175 **3.4. Upper Schist-Metagranitoid Unit: Serie Negra Group (Montemolín Formation)**

176 This unit comprises metasedimentary and metaigneous rocks, in which mafic,
177 intermediate, and felsic terms can be recognized. The metasedimentary series includes
178 schists, grey metagreywackes, black quartzites, and black schists. Black schists and
179 quartzites occur as decimeter- to meter-scale lenses within the other schists and
180 metagreywackes, while the latter are featured by cm- to mm-scale compositional layering
181 that alternates finer and coarser grained rocks (relict of sedimentary bedding).
182 Metabasites can be found as fine-grained, lens-shaped (meter-scale) bodies dispersed
183 over the metasedimentary series. Former regional studies identified this series as a
184 correlative to a section of the Serie Negra Group (Bandrés, 2001). Its primary immature
185 nature (as inferred from greywackic composition), along with its content in mafic rocks,
186 suggest it could be equivalent to the lower (and older) member of such group, regionally
187 referred to as Montemolín Formation (Eguíluz, 1987).

188 The sedimentary series was the host to a compositionally complex variety of
189 intrusive igneous rocks. The (finer-grained) metabasites cited above can be distinguished
190 from metagabbros that occur as coarser-grained rocks in larger patches and usually next
191 to metatonalites. Some metagabbros preserve a primary (equigranular) igneous texture.
192 Differences in grain size between the latter and fine-grained metabasites are not observed
193 in zones accumulating larger strain. Therefore, current differences in grain size may be
194 related to its primary texture (basalts/microgabbros vs. gabbros). Metatonalites,
195 metagranodiorites, and metagranites occur as variably strained, kilometer-scale bodies
196 within the metasedimentary rock series. Sections of these bodies accumulating more
197 strain can be observed as mafic, intermediate, or felsic orthogneisses, respectively,
198 whereas poorly strained sections show good exposures to analyze the primary texture of
199 their protoliths. Introducing details on the range of primary textures exceeds the purpose



200 of this contribution, but as a preliminary approach, all metagranitoids presented phaneritic
201 texture, ranging between fine- and coarse-grained, and showed either equigranular or
202 porphyritic terms (more common in felsic granitoids). Varied combinations of these
203 primary end-members plus heterogeneous strain explain the whole microstructural
204 variety observed in the metagranitoids of this unit, in which it can be recognized felsic
205 through to mafic metagranitoids with vaguely-defined planar fabric up to gneisses with
206 well-developed compositional banding or even augen (K-Feldspar) structure.

207 Being the most heterogeneous in lithological composition, this unit gathers
208 variably strained lithologies that resulted from metamorphic transformation of a rock
209 ensemble that included sedimentary and intrusive igneous rocks. None of the lithologies
210 listed above is separated from the rest ones within this unit by mechanical contacts with
211 crustal bearing, since no juxtaposition of lithologies with contrasting tectonothermal
212 evolution (see below) is observed. Therefore the whole ensemble represents a coherent
213 tectonic slice with continental affinity.

214

215 **3.5. Mafic-ultramafic Unit: Mérida Ophiolite**

216 The Mérida Massif contains an exposure of mafic and ultramafic rocks that have
217 been grouped into a single tectonostratigraphic unit due to its contrasting composition
218 and consistent structural position (see below) relative to surrounding lithologies. This unit
219 contains coarse-grained gabbros, pegmatitic gabbros, coarse-grained metagabbros,
220 amphibolites, garnet-bearing amphibolites, hornblendites, and serpentinites. It lacks of
221 felsic and intermediate igneous rocks, and of paraderived lithologies. No cross-cutting
222 relationships have been observed between pristine igneous rocks and the rest of
223 metamorphic rocks of this unit. In fact, some of the latter have been directly observed as
224 the result of variably strained sections of the first along discrete shear zones (e.g.



225 amphibolites after gabbros). Therefore the whole ensemble is considered as a
226 heterogeneously strained and variably recrystallized mafic-ultramafic complex.

227 Ultramafic rocks, such as strongly foliated serpentinites, occur at different levels
228 across structure within this unit. Poorly-strained gabbros allow inferring primary igneous
229 textures (will not be described here), none of which dominates over a particular structural
230 position across this unit. This mafic-ultramafic Unit shows outstanding ocean crust
231 affinity, and probably represents tectonic slices of lower oceanic crust and upper mantle
232 that will be collectively referred to as the Mérida Ophiolite.

233

234 **3.6. Lower Gneiss Unit: Magdalena Gneisses**

235 This unit consists of penetratively deformed and strongly recrystallized
236 metamorphic rocks. A preliminary study does not allow us to recognize between ortho-
237 and paraderived terms in it, being felsic rocks in all cases. They contain abundant quartz
238 and feldspar, although abundance in mica varies from one field exposure to the other.
239 Grain size is usually small (larger crystals in the matrix are 1-2 mm in size). Some
240 gneisses show lenticular grains that are slightly larger (2-3 mm) than the minerals in the
241 quartz-feldspathic matrix, whereas others contain mineral aggregates (mostly made of
242 quartz and feldspar) that show similar structure. The augen appearance for single-mineral
243 lenses could derive from a micro-porphyritic texture in the protolith, which could
244 tentatively be identified as igneous (granitoid?) in nature. Some of these gneisses include
245 green amphibole and biotite. Mica-rich and augen-free varieties in these gneisses are less
246 abundant and could represent paraderived rocks.

247 No mafic rocks were observed within these gneisses, as opposed to the rest of
248 units around. The absence of mafic rocks makes it difficult to interpret this ensemble as
249 a piece of either oceanic or transitional crust. Potential protoliths for the lithologies



250 grouped into this unit (sedimentary and felsic igneous rocks) represent typical
251 counterparts of continental crust *sensu lato*, although alternative options cannot be ruled
252 out due to the limited exposure of this unit.

253

254 4. REGIONAL STRUCTURE AND METAMORPHISM

255 The youngest regional structure of the Mérida Massif is a set of NE-dipping, high-
256 angle faults that cuts across the contacts of the Miocene sedimentary rocks (RP-1; Fig. 3)
257 and juxtaposes the crystalline basement onto some sections of the Cenozoic cover.
258 Tectonic transport is consistently to the SW. Displacement for all these thrusts, as
259 deduced from offsets in pre-fault lithological contacts, is quite limited, probably in the
260 range of tens of meters at most. Some of the sinuous trace of the basal contact of the
261 Cenozoic cover near these thrusts could be explained by very open folds, e.g. fault-
262 propagation folds, although no systematic measurement of bedding is available to prove
263 it. Besides such direct evidence of Alpine tectonics, it should be noted that most of the
264 exposure of the Mérida Massif occurs in a small peneplain that stands about 30-60 meters
265 above the areas located to the SW, S, and SE of the Guadiana river, whose trace in the
266 surroundings of Mérida town could be controlled by some other Alpine thrusts with
267 similar displacement (vertical offset at 30-60 meters) and kinematics (RP-2; Fig. 3)
268 (Vegas et al., 2012). The carbonated crusts, proposed to be Pleistocene-Holocene in age
269 (Insúa Márquez et al., 2003), affects both the Miocene deposits and the overriding
270 crystalline basement, thus suggesting a post-Miocene and pre-Pleistocene age (probably
271 Pliocene) for some Alpine thrusts in the region.

272 The Ordovician and pre-Ordovician rocks of the study area are separated by a SW-
273 dipping fault, the San Pedro thrust (RP-3; Fig. 3). Kinematics of this fault is top-to-the-
274 NE, and includes a left-lateral component that makes it an oblique-slip thrust (Gonzalo,



1987, 1989; Bandrés, 2001). Each block of this fault shows slightly different structural record. The internal structure of the footwall is dominated by Ordovician strata affected by NW-SE trending, upright to NE-verging overturned folds (Cornalvo synform), to which local, and single, main foliation is axial planar (Fig. 4a). There, strata is duplicated and folds are cut by SW-dipping thrusts with moderate offset, which probably represent minor fault imbricates of the San Pedro thrust. The internal structure of the hanging wall to the San Pedro thrust is defined by rocks showing a main foliation affected by NW-SE trending, upright to either NE- or SW-verging overturned folds (Figs. 3 and 4a). SW-verging folds are scarcer and tend to occur around a NE-dipping thrust that cuts across the internally folded structure of the upper block to the San Pedro fault, which will be referred to as the Barranca back-thrust (RP-4; Fig. 3). The main foliation usually runs parallel to the boundaries of the bodies of metagranitoids that can be observed in the Upper Schist-Metagranitoid Unit. The Lower Gneiss Unit crops out in the core of a dome-like fold, the Magdalena antiform or dome (RP-5; Fig. 3), while the Cambrian marbles occupy the core of a synform paired with the Magdalena antiform, here referred to as the Carija synform (RP-6; Fig. 3). Using the main foliation as reference, the structure of the pre-Ordovician units would consist of a tectonic pile with the Lower Gneiss Unit resting below the Mérida Ophiolite, which would be covered by the Schist-Metagranitoid Unit (Ediacaran Serie Negra Group) and then the Carija Unit (Cambrian marbles) (cross-section in Fig. 4b).

The traces of the contacts between tectonostratigraphic units in the hanging wall to the San Pedro thrust are featured by mylonites. As a preliminary description, the contact between the Upper Schist-Metagranitoid Unit and the Mérida Ophiolite is defined by a ductile shear zone that includes a shear band with mylonites (after mafic and ultramafic rocks, metasedimentary rocks and metagranites) located at the boundary



300 between tectonostratigraphic units (core of a major shear zone), and a set of variably
301 strained rocks towards more distal sections (Trujillanos detachment). Kinematic criteria
302 indicate consistent top-to-the-SSE shear sense. The contact between the Mérida Ophiolite
303 and the Lower Gneiss Unit is also featured by mylonites (Magdalena thrust). A
304 preliminary kinematic analysis of this contact provided no consistent results, probably
305 due to a more complex nature compared to that of other major boundaries in the region
306 (see discussion section). The contact between the Upper Schist-Metagranitoid Unit and
307 the Carija Unit is marked by mylonites after limestones and siliciclastic rocks (black calc-
308 schists) (Carija detachment). Kinematic criteria indicate a consistent top-to-the-NNW
309 sense of shear. The trace of all of these contacts shows sinuous pattern and run roughly
310 parallel to the main foliation observed in the hanging wall to the San Pedro thrust, both
311 (foliation and mechanical contacts) defining the same NE-SW trending folds (Fig. 4a).

312 Strain and metamorphic recrystallization is heterogeneous, but the metamorphic
313 grade varies vertically across structure. The mineral assemblages of the main foliation in
314 the hanging wall to the San Pedro thrust defines an overall normal metamorphic gradient.
315 As a reference, the main foliation in the metasedimentary rocks of the Upper Schist-
316 Metagranitoid Unit may include quartz, plagioclase, white mica, biotite, and minor
317 (secondary?) chlorite, which make a typical greenschist facies fabric (probably in the
318 biotite zone). The main foliation in the mafic rocks of that unit includes plagioclase, fine-
319 grained green amphibole, zoisite, epidote, titanite and chlorite, an assemblage also
320 compatible with greenschist facies conditions. The main foliation in the mafic rocks of
321 the Mérida Ophiolite is defined by plagioclase, brown-green amphibole (hornblende),
322 titanite, opaques, and minor rutile. Some exposures include large garnet porphyroblasts,
323 and altogether define a typical assemblage for amphibolite facies conditions (grain-size
324 for the meta-mafic rocks in this unit is significantly larger than in the Upper Schist-



325 Metagranitoid Unit). PT conditions for this assemblage were estimated at 1.2 GPa and
326 750 °C (Bandrés et al., 2000). The main foliation in the Lower Gneiss Unit includes
327 recrystallized plagioclase, K-feldspar, green amphibole, biotite and quartz ribbons with
328 granoblastic polygonal texture. This fabric is occasionally accompanied by patches of
329 melt crystallized along bands parallel to the main foliation. The regional normal gradient
330 in the hanging wall to the San Pedro thrust is juxtaposed onto Ordovician strata, which
331 show a penetrative slaty cleavage formed by quartz, white mica, chlorite, sericite and
332 opaques (chlorite zone).

333

334 **5. DISCUSSION AND PRELIMINARY CONCLUSIONS**

335 Alpine deformation in the Mérida Massif is limited and mostly restricted to high-
336 angle thrusts that reworked its crystalline basement and faulted its Cenozoic cover (at
337 least during the Pliocene). Main shortening direction is NE-SW and dominant tectonic
338 transport for thrusts is to the SW. Given the distal position to Cenozoic plate boundaries,
339 this deformation can be framed into an intra-plate setting for the Iberian micro-plate (e.g.,
340 de Vicente and Vegas, 2009).

341 The NW-SE trending folds that affect the basement of the Mérida Massif represent
342 the first deformation for the Ordovician strata, but are at least the second pulse of
343 deformation taken by the entire set of pre-Ordovician rocks (note their main foliation and
344 ductile shear zones are affected by these folds). This indicates that these folds, and the
345 faults they are cut by (San Pedro and Barranca thrusts) are Variscan in age, and that the
346 main foliation and ductile shear zones in the pre-Ordovician rocks are probably pre-
347 Variscan and responsible for the layered structure of most of the tectonostratigraphic
348 units. This pre-Variscan age of deformation is also supported by Sm-Nd dating of
349 metamorphic garnet growth in the metabasites of the Mérida Ophiolite (555 Ma; Bandrés



350 et al., 2004). As a consequence, the current contacts between tectonostratigraphic units in
351 the hanging wall to the San Pedro thrust could be framed in a Cadomian setting. Normal
352 metamorphic gradient within and around their juxtaposed tectonic blocks, together with
353 their crustal-scale bearing (they juxtaposed sections with different metamorphic imprint),
354 suggest they represent large-scale extensional shear zones. The current folded structure
355 of these shear zones favors a primary flat-lying geometry for all of them, so they should
356 be referred to as extensional detachments. The Carija detachment affects Cambrian strata,
357 so the functioning of some of them may be restricted to the Cambrian and perhaps
358 Ordovician.

359 The current regional boundaries between all of the pre-Ordovician
360 lithostratigraphic units are mechanical in nature, so there is no reason to consider the
361 entire set of basement rocks as a single tectonic block prior to Ordovician times. Some of
362 these contacts reflected the functioning of rather different faults through time, what may
363 explain part of their kinematic complexity observed in a preliminary analysis. The Mafic-
364 Ultramafic Unit of the Mérida Massif separates two lithological ensembles that show
365 continental crust affinity, the Mérida Ophiolite being an exposure of a suture zone. Should
366 the current upper boundary of the Mérida Ophiolite be a pre-Ordovician extensional fault
367 (Trujillanos detachment), the suture zone this mafic-ultramafic unit represents must be
368 Cadomian in age. The current juxtaposition of tectonostratigraphic units in the Mérida
369 Massif suggests a large-scale nappe structure for this suture, where the Lower Gneiss Unit
370 would represent the lower plate, and the Mérida Ophiolite would account for oceanic
371 lithosphere located at the base of the upper plate, here represented by the Upper Schist-
372 Metagranitoid Unit. This way, the primary upper and lower boundaries of the Mérida
373 Ophiolite could be Cadomian accretionary thrusts, the current nappe structure being the
374 result of a late Cadomian extensional event that operated over previously thickened crust



375 built at the expense of basal tectonic accretion (peak metamorphic conditions for the
376 Mérida Ophiolite suggest lower crust depth). The root of the suture zone represented by
377 the Mérida Ophiolite is not exposed in the study area, as its lower plate (Lower Gneiss
378 Unit) occurs in a tectonic window. This supports a pre-Variscan low-dipping geometry
379 for the thrust sheets involved in the suture zone (e.g. Magdalena thrust; Fig. 4b), some of
380 the tectonostratigraphic units being actual allochthonous terranes.

381 The sequence and broad timing of tectonic events recognized for the building of
382 Mérida Massif fit well into the regional geology of SW Iberia. The Cadomian suture zone
383 and nappe structure identified in the Mérida Massif add to the evidence of Cadomian
384 tectonics in southern Europe (Eguíluz et al., 2001; Díez Fernández et al., 2019; Quesada,
385 1990; Simancas et al., 2004; Pereira et al., 2012; Díaz García, 2006; Pieren et al., 1987;
386 Bandres et al., 2002), which is tightly connected to subduction-accretion processes in the
387 periphery of the African margin of Gondwana (Orejana et al., 2015; Fuenlabrada et al.,
388 2012; Rojo-Pérez et al., 2019; Arenas et al., 2018; Sánchez Lorda et al., 2014; Linnemann
389 et al., 2008; Bandrés et al., 2004). Variscan deformation in the Mérida Massif reworked
390 but did not reactivate major Cadomian structures such as accretionary faults and
391 extensional detachments, which are now observed as folded planes cut at high-angle by
392 Variscan major faults. In this regard, late Cadomian extension can be observed as a
393 transitional stage to the Variscan cycle, but most importantly, as a contributor to the
394 stabilization (cratonization) of orogenic crust before subsequent deformation.

395 The gathering of contrasting individual lithologies into tectonostratigraphic units
396 is proven here as a powerful tool to identify major tectonic blocks in orogeny, even at the
397 lithosphere scale. Equivalent approaches performed in other areas of the Iberian Massif
398 before focused mostly on the identification of major Variscan thrust sheets (Ribeiro et al.,
399 2010; Ries and Shackleton, 1971; Díez Fernández and Arenas, 2015; Arenas et al., 1986).



400 Our work presents a case example that proves this method right for Cadomian tectonics,
401 and adds evidence to the notion that the lithosphere of the Iberian micro-plate was
402 constructed not only by the functioning of large-scale accretionary faults and tectonic
403 transport of allochthonous terranes during the Variscan Orogeny (e.g., Martínez Catalán
404 et al., 2009; Díez Fernández et al., 2016; Ribeiro et al., 2007), but also during the
405 Cadomian Orogeny (e.g., Díez Fernández et al., 2019; Abalos et al., 1991).

406

407 **6. DATA AVAILABILITY**

408 The data is directly accessible through the published text and figures.

409

410 **7. AUTHOR CONTRIBUTION**

411 RDF, RA and ERP designed the mapping campaign and carried it out. RDF
412 delineated the maps (Figures 2 and 3) and draw the cross-sections (Figure 4). All authors
413 discussed and interpreted the data and prepared the manuscript.

414

415 **8. COMPETING INTERESTS**

416 The authors declare that they have no conflict of interest.

417

418 **9. ACKNOWLEDGMENTS**

419 Research funded by Spanish project CGL2016-76438-P (Ministerio de Economía,
420 Industria y Competitividad).

421

422 **10. REFERENCES CITED**



- 423 Abalos, B., Gil Iburguchi, J. I., and Eguiluz, L.: Cadomian subduction, collision and
424 Variscan transpression in the Badajoz-Cordoba Shear Belt, Southwest Spain,
425 Tectonophysics, 199, 51-72, 1991.
- 426 Arenas, R., Gil Iburguchi, J. I., González Lodeiro, F., Klein, E., Martínez Catalán, J. R.,
427 Ortega Gironés, E., Pablo Maciá, J. G. d., and Peinado, M.: Tectonostratigraphic
428 units in the complexes with mafic and related rocks of the NW of the Iberian
429 Massif, Hercynica, 2, 87-110, 1986.
- 430 Arenas, R., Fernández-Suárez, J., Montero, P., Díez Fernández, R., Andonaegui, P.,
431 Sánchez Martínez, S., Albert, R., Fuenlabrada, J. M., Matas, J., Martín Parra, L.
432 M., Rubio Pascual, F. J., Jiménez-Díaz, A., and Pereira, M. F.: The Calzadilla
433 Ophiolite (SW Iberia) and the Ediacaran fore-arc evolution of the African margin
434 of Gondwana, Gondwana Research, 58, 71-86, 10.1016/j.gr.2018.01.015, 2018.
- 435 Azor, A., Lodeiro, F. G., and Simancas, J. F.: Tectonic evolution of the boundary between
436 the Central Iberian and Ossa-Morena zones (Variscan belt, southwest Spain),
437 Tectonics, 13, 45-61, 10.1029/93tc02724, 1994.
- 438 Balé, P., and Brun, J. P.: Late Precambrian thrust and wrench zones innorthern Brittany
439 (France), Journal of Structural Geology, 11, 391-405, 1989.
- 440 Ballèvre, M., Bosse, V., Ducassou, C., and Pitra, P.: Palaeozoic history of the Armorican
441 Massif: Models for the tectonic evolution of the suture zones, Comptes Rendus
442 Geoscience, 341, 174-201, 10.1016/j.crte.2008.11.009, 2009.
- 443 Bandres, A., Eguíluz, L., Iburguchi, J. I. G., and Palacios, T.: Geodynamic evolution of a
444 Cadomian arc region: the northern Ossa-Morena zone, Iberian massif,
445 Tectonophysics, 352, 105-120, 10.1016/S0040-1951(02)00191-9, 2002.
- 446 Bandrés, A., Eguiluz, L., Menéndez, M., Ortega, L. A., and Gil Iburguchi, J. I.: El macizo
447 precámbrico de Mérida (suroeste de España): petrografía, geoquímica,



- 448 geocronología y significado geodinámico, *Cadernos del Laboratorio Xeológico de*
449 *Laxe*, 25, 159-163, 2000.
- 450 Bandrés, A.: Evolución geodinámica poliorogénica de los Dominios septentrionales de la
451 Zona Ossa-Morena, Universidad del País Vasco, 377 pp., 2001.
- 452 Bandrés, A., Eguíluz, L., Pin, C., Paquette, J. L., Ordóñez, B., Le Fèvre, B., Ortega, L.
453 A., and Gil Ibarguchi, J. I.: The northern Ossa-Morena Cadomian batholith
454 (Iberian Massif): magmatic arc origin and early evolution, *International Journal*
455 *of Earth Sciences*, 93, 860-885, 10.1007/s00531-004-0423-6, 2004.
- 456 Chantraine, J., Egal, E., Thiéblemont, D., Le Goff, E., Guerrot, C., Ballèvre, M., and
457 Guennoc, P.: The Cadomian active margin (North Armorican Massif, France): a
458 segment of the North Atlantic Panafrican belt, *Tectonophysics*, 331, 1-18,
459 10.1016/s0040-1951(00)00233-x, 2001.
- 460 D’Lemos, R. S., Strachan, R. A., and Topley, C. G.: The Cadomian Orogeny, *Geological*
461 *Society of London, Special Publications*, 423 pp., 1990.
- 462 de Vicente, G., and Vegas, R.: Large-scale distributed deformation controlled topography
463 along the western Africa–Eurasia limit: Tectonic constraints, *Tectonophysics*,
464 474, 124-143, 10.1016/j.tecto.2008.11.026, 2009.
- 465 de Vicente, G., Cunha, P. P., Muñoz-Martín, A., Cloetingh, S. A. P. L., Olaiz, A., and
466 Vegas, R.: The Spanish-Portuguese Central System: An Example of Intense
467 Intraplate Deformation and Strain Partitioning, *Tectonics*, 37, 4444-4469,
468 10.1029/2018tc005204, 2018.
- 469 Dewey, J. F., Helman, M. L., Turco, E., Hutton, D. H. W., and Knot, S. D.: Kinematics
470 of the western Mediterranean, *Geological Society of London Special Publication*,
471 45, 265-283, 1989.



- 472 Díaz García, F.: Geometry and regional significance of Neoproterozoic (Cadomian)
473 structures of the Narcea Antiform, NW Spain, *Journal of the Geological Society*,
474 163, 499-508, 10.1144/0016-764905-090, 2006.
- 475 Díez Fernández, R., and Arenas, R.: The Late Devonian Variscan suture of the Iberian
476 Massif: A correlation of high-pressure belts in NW and SW Iberia,
477 *Tectonophysics*, 654, 96-100, 10.1016/j.tecto.2015.05.001, 2015.
- 478 Díez Fernández, R., Arenas, R., Pereira, M. F., Sánchez Martínez, S., Albert, R., Martín
479 Parra, L. M., Rubio Pascual, F. J., and Matas, J.: Tectonic evolution of Variscan
480 Iberia: Gondwana - Laurussia collision revisited, *Earth-Science Reviews*, 162,
481 269-292, 10.1016/j.earscirev.2016.08.002, 2016.
- 482 Díez Fernández, R., Jiménez-Díaz, A., Arenas, R., Pereira, M. F., and Fernández-Suárez,
483 J.: Ediacaran Obduction of a Fore-arc Ophiolite in SW Iberia: A Turning Point in
484 the Evolving Geodynamic Setting of Peri-Gondwana, *Tectonics*, 38, 95-119,
485 10.1029/2018TC005224, 2019.
- 486 Díez Fernández, R., Matas, J., Arenas, R., Martín-Parra, L. M., Sánchez Martínez, S.,
487 Novo-Fernández, I., and Rojo-Pérez, E.: Two-step obduction of the Porvenir
488 Serpentinite: a cryptic Devonian suture in SW Iberian Massif (Ossa-Morena
489 Complex), in: *Special Paper in honor of Eldridge M. Moores*, edited by:
490 Wakabayashi, J., Dilek, Y., and Ogawa, Y., GSA Books, in press.
- 491 Dorr, W., Zulauf, G., Fiala, J., Franke, W., and Vejnar, Z.: Neoproterozoic to Early
492 Cambrian history of an active plate margin in the Tepla-Barrandian unit - a
493 correlation of U-Pb isotopic-dilution-TIMS ages (Bohemia, Czech Republic),
494 *Tectonophysics*, 352, 65-85, 2002.
- 495 Drost, K., Linnemann, U., McNaughton, N., Fatka, O., Kraft, P., Gehmlich, M., Tonk,
496 C., and Marek, J.: New data on the Neoproterozoic - Cambrian geotectonic setting



- 497 of the Tepla-Barrandian volcano-sedimentary successions: geochemistry, U-Pb
498 zircon ages, and provenance (Bohemian Massif, Czech Republic), *International*
499 *Journal of Earth Sciences*, 93, 742-757, 10.1007/s00531-004-0416-5, 2004.
- 500 Eguíluz, L.: Petrogénesis de rocas ígneas y metamórficas en el Antiforme Burguillos-
501 Monesterio, Macizo Ibérico Meridional, Universidad del País Vasco, 694 pp.,
502 1987.
- 503 Eguíluz, L., Gil Ibarguchi, J. I., Abalos, B., and Apraiz, A.: Superposed Hercynian and
504 Cadomian orogenic cycles in the Ossa-Morena zone and related areas of the
505 Iberian Massif, *Geological Society of America Bulletin*, 112, 1398-1413,
506 10.1130/0016-7606(2000)112<1398:SHACOC>2.0.CO;2, 2000.
- 507 Eguíluz, L., Bandrés, A., Ortega, J. L., Gil Ibarguchi, J. I., Garcés, M., Paquette, J. L.,
508 and Pin, C.: New evidence on the Cadomian evolution of northern Ossa-Morena
509 zone (SW Spain), *Collisional Orogens, Annual Meeting of the IGCP 453*, 2001,
510 67-68,
- 511 Expósito, I., Simancas, J. F., González Lodeiro, F., Bea, F., Montero, P., and Salman, K.:
512 Metamorphic and deformational imprint of Cambrian-Lower Ordovician rifting
513 in the Ossa-Morena Zone (Iberian Massif, Spain), *Journal of Structural Geology*,
514 25, 2077-2087, 10.1016/s0191-8141(03)00075-0, 2003.
- 515 Fernández-Suárez, J., Gutiérrez-Alonso, G., Pastor-Galán, D., Hofmann, M., Murphy, J.
516 B., and Linnemann, U.: The Ediacaran–Early Cambrian detrital zircon record of
517 NW Iberia: possible sources and paleogeographic constraints, *International*
518 *Journal of Earth Sciences*, 1-23, 10.1007/s00531-013-0923-3, 2013.
- 519 Franke, W.: The mid-European segment of the Variscides: Tectonostratigraphic units,
520 terrane boundaries and plate tectonic evolution, in: *Orogenic Processes:*
521 *Quantification and Modelling in the Variscan Belt*, edited by: Franke, W., Haak,



- 522 V., Oncken, O., and Tanner, D., Geological Society, London, Special
523 Publications, 35-61, doi: 10.1144/GSL.SP.2000.1179.1101.1105, 2000.
- 524 Fuenlabrada, J. M., Arenas, R., Díez Fernández, R., Sánchez Martínez, S., Abati, J., and
525 López Carmona, A.: Sm–Nd isotope geochemistry and tectonic setting of the
526 metasedimentary rocks from the basal allochthonous units of NW Iberia (Variscan
527 suture, Galicia), *Lithos*, 148, 196-208, 10.1016/j.lithos.2012.06.002, 2012.
- 528 Fuenlabrada, J. M., Pieren, A. P., Díez Fernández, R., Sánchez Martínez, S., and Arenas,
529 R.: Geochemistry of the Ediacaran-Early Cambrian transition in Central Iberia:
530 Tectonic setting and isotopic sources, *Tectonophysics*, 681, 15-30,
531 10.1016/j.tecto.2015.11.013, 2016.
- 532 Gonzalo, J. C.: Petrología y estructura del Basamento en el área de Mérida (Extremadura
533 Central), PhD, Universidad de Salamanca, 327 pp., 1987.
- 534 Gonzalo, J. C.: Litoestratigrafía y tectónica del basamento en el área de Mérida
535 (Extremadura Central), *Boletín Geológico y Minero*, 100-1, 48-72, 1989.
- 536 Gutiérrez-Marco, J. C., Robardet, M., Rábano, I., Sarmiento, G. N., San José Lancha, M.
537 A., Herranz Araujo, P., and Pieren Pidal, A. P.: Ordovician, in: *The Geology of*
538 *Spain*, edited by: Gibbons, W., and Moreno, T., Geological Society of London,
539 London, 31-49, 2002.
- 540 Henriques, S. B. A., Neiva, A. M. R., Ribeiro, M. L., Dunning, G. R., and Tajčmanová,
541 L.: Evolution of a Neoproterozoic suture in the Iberian Massif, Central Portugal:
542 New U-Pb ages of igneous and metamorphic events at the contact between the
543 Ossa Morena Zone and Central Iberian Zone, *Lithos*, 220–223, 43-59,
544 10.1016/j.lithos.2015.02.001, 2015.
- 545 Insúa Márquez, M., López Sopena, F., Hernández Samaniego, A., Matia Villarino, G.,
546 Ortega Ruiz, I., Pascual Martínez, E., Agudo Fernández, L., de la Fuente Krauss,



- 547 J. V., Martín Duque, J. F., Moreno, F., Carvajal, A., Cantos Robles, R., Liñán
548 Guijarro, E., Fernández-Gianotti, J., Gabaldón, V., Rubio, J. C., and Baeza, L. J.:
549 Mapa Geológico y Memoria explicativa, Hoja 777 (Mérida), Serie MAGNA,
550 1/50.000, Instituto Geológico y Minero de España, 2003.
- 551 Jolivet, L., Augier, R., Faccenna, C., Negro, F., Rimmerle, G., Agard, P., Robin, C.,
552 Rossetti, F., and Crespo-Blanc, A.: Subduction, convergence and the mode of
553 backarc extension in the Mediterranean region, *Bulletin de la Societe Geologique*
554 *de France*, 179, 525-550, 10.2113/gssgfbull.179.6.525, 2008.
- 555 Kröner, A., Štípská, P., Schulmann, K., and Jaeckel, P.: Chronological constraints on the
556 pre-Variscan evolution of the northeastern margin of the Bohemian Massif, Czech
557 Republic, *Geological Society, London, Special Publications*, 179, 175-197,
558 10.1144/GSL.SP.2000.179.01.12, 2000.
- 559 Linnemann, U., Gehmlich, M., Tichomirowa, M., Buschmann, B., Nasdala, L., Jonas, P.,
560 Lützner, H., and Bombach, K.: From Cadomian subduction to Early Paleozoic
561 rifting: The evolution of Saxo-Thuringia at the margin of Gondwana in the light
562 of single zircon geochronology and basin development (central European
563 Variscides, Germany), *Geological Society, London, Special Publications*, 179,
564 131-153, 2000.
- 565 Linnemann, U., Gerdes, A., Drost, K., and Buschmann, B.: The continuum between
566 Cadomian orogenesis and opening of the Rheic Ocean: Constraints from LA-ICP-
567 MS U–Pb zircon dating and analysis of plate-tectonic setting (Saxo-Thuringian
568 zone, northeastern Bohemian Massif, Germany), in: *The evolution of the Rheic*
569 *Ocean: From Avalonian-Cadomian active margin to Alleghenian-Variscan*
570 *collision*, edited by: Linnemann, U., Nance, R. D., Kraft, P., and Zulauf, G.,



- 571 Geological Society of America Special Paper, 61-96, doi:
572 10.1130/2007.2423(1103), 2007.
- 573 Linnemann, U., Pereira, F., Jeffries, T. E., Drost, K., and Gerdes, A.: The Cadomian
574 Orogeny and the opening of the Rheic Ocean: The diachrony of geotectonic
575 processes constrained by LA-ICP-MS U–Pb zircon dating (Ossa-Morena and
576 Saxo-Thuringian Zones, Iberian and Bohemian Massifs), *Tectonophysics*, 461,
577 21-43, 10.1016/j.tecto.2008.05.002, 2008.
- 578 Martínez Catalán, J. R., Arenas, R., Abati, J., Sánchez Martínez, S., Díaz García, F.,
579 Fernández-Suárez, J., González Cuadra, P., Castiñeiras, P., Gómez Barreiro, J.,
580 Díez Montes, A., González Clavijo, E., Rubio Pascual, F. J., Andonaegui, P.,
581 Jeffries, T. E., Alcock, J. E., Díez Fernández, R., and López Carmona, A.: A
582 rootless suture and the loss of the roots of a mountain chain: The Variscan belt of
583 NW Iberia, *Comptes Rendus Geoscience*, 341, 114-126,
584 10.1016/j.crte.2008.11.004, 2009.
- 585 Matte, P.: Accretionary history and crustal evolution of the Variscan belt in Western
586 Europe, *Tectonophysics*, 196, 309-337, 1991.
- 587 Nance, R. D., Murphy, J. B., Strachan, R. A., D'Lemos, R. S., and Taylor, G. K.: Late
588 Proterozoic tectonostratigraphic evolution of the Avalonian and Cadomian
589 terranes, *Precambrian Research*, 53, 41-78, 1991.
- 590 Nance, R. D., Gutiérrez-Alonso, G., Keppie, J. D., Linnemann, U., Murphy, J. B.,
591 Quesada, C., Strachan, R. A., and Woodcock, N. H.: Evolution of the Rheic
592 Ocean, *Gondwana Research*, 17, 194-222, 10.1016/j.gr.2009.08.001, 2010.
- 593 Orejana, D., Martínez, E. M., Villaseca, C., and Andersen, T.: Ediacaran–Cambrian
594 paleogeography and geodynamic setting of the Central Iberian Zone: Constraints



- 595 from coupled U–Pb–Hf isotopes of detrital zircons, *Precambrian Research*, 261,
596 234-251, 10.1016/j.precamres.2015.02.009, 2015.
- 597 Pereira, M. F., Silva, J. B., Chichorro, M., Moita, P., Santos, J. F., Apraiz, A., and Ribeiro,
598 C.: Crustal growth and deformational processes in the northern Gondwana
599 margin: Constraints from the Évora Massif (Ossa-Morena Zone, southwest Iberia,
600 Portugal), in: *The evolution of the Rheic Ocean: From Avalonian-Cadomian
601 active margin to Alleghenian-Variscan collision*, edited by: Linnemann, U.,
602 Nance, R. D., Kraft, P., and Zulauf, G., *Geological Society of America Special
603 Paper*, 333-358, doi: 310.1130/2007.2423(1116), 2007.
- 604 Pereira, M. F., Solá, A. R., Chichorro, M., Lopes, L., Gerdes, A., and Silva, J. B.: North-
605 Gondwana assembly, break-up and paleogeography: U–Pb isotope evidence from
606 detrital and igneous zircons of Ediacaran and Cambrian rocks of SW Iberia,
607 *Gondwana Research*, 22, 866 - 881, 10.1016/j.gr.2012.02.010, 2012.
- 608 Pereira, M. F.: Potential sources of Ediacaran strata of Iberia: a review, *Geodinamica
609 Acta*, 27, 1-14, 10.1080/09853111.2014.957505, 2015.
- 610 Pieren, A. P., Pineda, A., and Herranz, P.: Discordancia intraprecámbrica en el anticlinal
611 de Agudo (Ciudad Real-Badajoz), *Geogaceta*, 2, 26-29, 1987.
- 612 Quesada, C.: Precambrian successions in SW Iberia: their relationship to ‘Cadomian’
613 orogenic events, in: *The Cadomian Orogeny*, edited by: Lemos, D. R., Strachan,
614 R. A., and Topley, C. G., *Geological Society, London, Special Publication*,
615 *Geological Society, London, Special Publication*, 353-362, 1990.
- 616 Ribeiro, A., Munhá, J., Dias, R., Mateus, A., Pereira, E., Ribeiro, L., Fonseca, P., Araújo,
617 A., Oliveira, T., Romão, J., Chaminé, H., Coke, C., and Pedro, J.: Geodynamic
618 evolution of the SW Europe Variscides, *Tectonics*, 26, TC6009,
619 10.1029/2006tc002058, 2007.



- 620 Ribeiro, A., Munhá, J., Fonseca, P. E., Araújo, A., Pedro, J. C., Mateus, A., Tassinari, C.,
621 Machado, G., and Jesus, A.: Variscan ophiolite belts in the Ossa-Morena Zone
622 (Southwest Iberia): Geological characterization and geodynamic significance,
623 *Gondwana Research*, 17, 408-421, 10.1016/j.gr.2009.09.005, 2010.
- 624 Ries, A. C., and Shackleton, R. M.: Catazonal Complexes of North-West Spain and North
625 Portugal, Remnants of a Hercynian Thrust Plate, *Nature Physical Science*, 234,
626 65-79, 10.1038/physci234065a0, 1971.
- 627 Rojo-Pérez, E., Arenas, R., Fuenlabrada, J. M., Sánchez Martínez, S., Martín Parra, L.
628 M., Matas, J., Pieren, A. P., and Díez Fernández, R.: Contrasting isotopic sources
629 (Sm-Nd) of Late Ediacaran series in the Iberian Massif: Implications for the
630 Central Iberian-Ossa Morena boundary, *Precambrian Research*, 324, 194-207,
631 10.1016/j.precamres.2019.01.021, 2019.
- 632 Roso de Luna, I., and Hernández Pacheco, F.: Mapa y memoria explicativa de la Hoja
633 1:50.000 n° 777 (Mérida) del Mapa Geológico de España (IGME), Instituto
634 Geológico y Minero de España, 1950.
- 635 Rubio-Ordóñez, A., Gutiérrez-Alonso, G., Valverde-Vaquero, P., Cuesta, A., Gallastegui,
636 G., Gerdes, A., and Cárdenes, V.: Arc-related Ediacaran magmatism along the
637 northern margin of Gondwana: Geochronology and isotopic geochemistry from
638 northern Iberia, *Gondwana Research*, 27, 216-227, 10.1016/j.gr.2013.09.016,
639 2015.
- 640 Sánchez-García, T., Bellido, F., Pereira, M. F., Chichorro, M., Quesada, C., Pin, C., and
641 Silva, J. B.: Rift-related volcanism predating the birth of the Rheic Ocean (Ossa-
642 Morena zone, SW Iberia), *Gondwana Research*, 17, 392-407,
643 10.1016/j.gr.2009.10.005, 2010.



- 644 Sánchez Lorda, M. E., Sarrionandia, F., Ábalos, B., Carracedo, M., Eguíluz, L., and Gil
645 Ibarguchi, J. I.: Geochemistry and paleotectonic setting of Ediacaran metabasites
646 from the Ossa-Morena Zone (SW Iberia), *International Journal of Earth Sciences*,
647 103, 1263-1286, 10.1007/s00531-013-0937-x, 2014.
- 648 Simancas, F., Expósito, I., Azor, A., Martínez Poyatos, D., and González Lodeiro, F.:
649 From the Cadomian orogenesis to the Early Palaeozoic Variscan rifting in
650 Southwest Iberia, *Journal of Iberian Geology*, 30, 53-71, 2004.
- 651 Simancas, J. F., Ayarza, P., Azor, A., Carbonell, R., Martínez Poyatos, D., Pérez-Estaún,
652 A., and González Lodeiro, F.: A seismic geotraverse across the Iberian Variscides:
653 Orogenic shortening, collisional magmatism, and orocline development,
654 *Tectonics*, 32, 417-432, 10.1002/tect.20035, 2013.
- 655 Strachan, R. A., and Taylor, G. K.: *Avalonian and Cadomian Geology of the North*
656 *Atlantic*, edited by: Blackie, London, 252 pp., 1990.
- 657 Vegas, R., Antón, L., Gomes, A., and Medialdea, T.: Lineaments in the West-Central
658 Hesperic Massif (Portugal and Spain) and their geomorphic and tectonic
659 significance, *Geo-Temas*, 13, 1674-1677, 2012.

660

661

662 **FIGURE CAPTION**

663 Figure 1: Zonation of the Variscan Orogen after Díez Fernández and Arenas (2015).

664 Location of the study area is indicated. Location of map in Figure 2 is indicated.

665 Figure 2: Regional geological map of the Obejo-Valsequillo Domain (Díez Fernández et

666 al., in press) showing the location of the Mérida Massif. Location of map in Figure 3 is

667 indicated.



668 Figure 3: Geological map showing the distribution of tectonostratigraphic units of the
669 Mérida Massif.

670 Figure 4: Cross sections showing the current structure of the tectonostratigraphic units of
671 the Mérida Massif. (a) Cross section normal to the trace of Variscan folds and faults. (b)
672 Cross section subparallel to shear direction of Cadomian shear zones and showing the
673 Cadomian nappe pile of the Mérida Massif. Cenozoic cover is not represented.

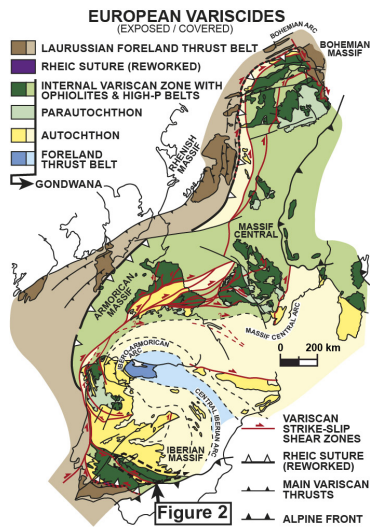
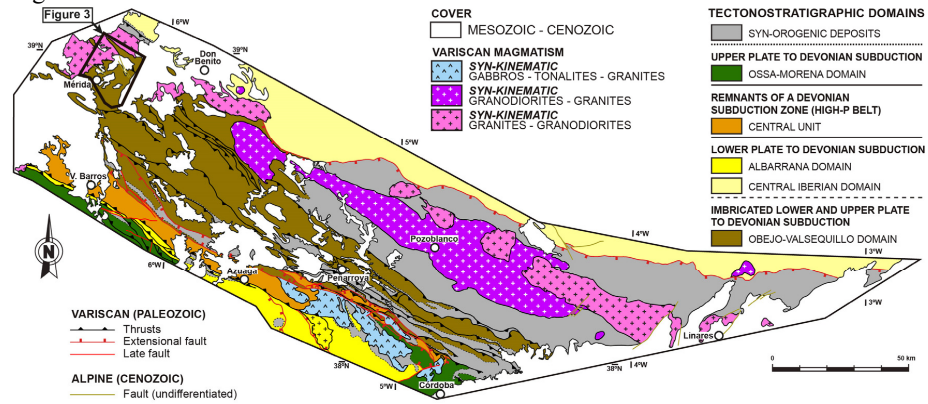


Figure 1



Figure 2



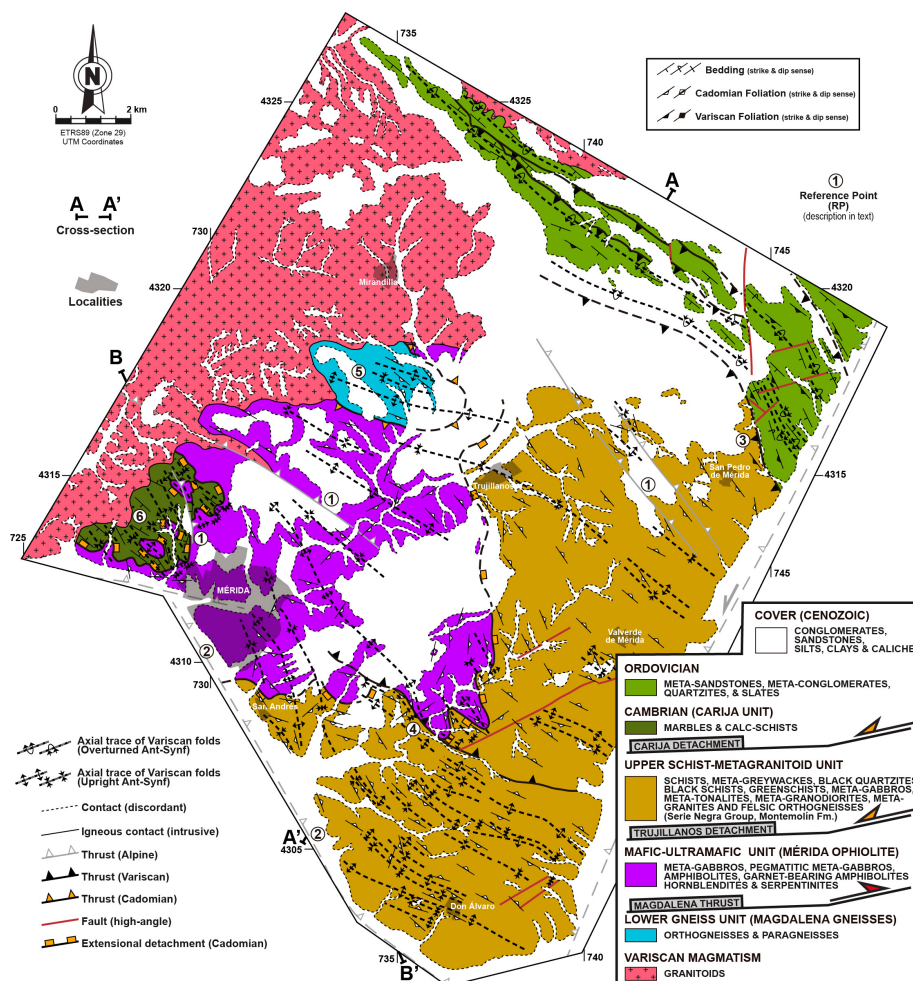


Figure 3



Figure 4

